BIOMOLECULES & THERAPEUTICS

Original Article
Biomol Ther 33(3), 501-509 (2025)

Hepatoprotective Effects of Resveratrol on Acetaminophen-Induced Acute Liver Injury and Its Implications for Tofacitinib Disposition in Rats

Hyeon Gyeom Choi[1], So Yeon Park[2], Sung Hun Bae[1], Sun-Young Chang[1,2] and So Hee Kim[1,2,*]

[1]College of Pharmacy and Research Institute of Pharmaceutical Science and Technology, Ajou University, Suwon 16499,
[2]Department of Biohealth Regulatory Science, Graduate School of Ajou University, Suwon 16499, Republic of Korea

Abstract

Tofacitinib, which is used to treat rheumatoid arthritis (RA), is primarily metabolized by the hepatic cytochrome P450 (CYP) enzymes, CYP3A1/2 and CYP2C11. Acetaminophen (APAP), which is frequently used for pain relief in patients with RA, can induce acute liver injury (ALI) when taken in excess, profoundly affecting drug metabolism. Resveratrol (RVT) is a polyphenolic compound with hepatoprotective properties. This study investigated the protective effects of RVT against APAP-induced ALI in rats, and explored its influence on the pharmacokinetics of tofacitinib. In ALI rats, both intravenous and oral administration of tofacitinib resulted in a significant (207% and 181%) increase in the area under the plasma concentration-time curve (AUC), primarily driven by a substantial reduction (66.1%) in non-renal clearance (CL_{NR}) compared to that in control (CON) rats. Notably, RVT administration in ALI rats provided effective liver protection, partially restoring liver function, as evidenced by normalized glutamate oxaloacetate transaminase levels and the pharmacokinetic parameters, AUC and CL_{NR}, closer to those observed in untreated CON rats (117% and 81.9%, respectively). These findings highlight the importance of considering the potential interactions between RVT or polyphenol-rich natural products and medications in patients with ALI in clinical practice.

Key Words: Tofacitinib, Acute liver injury, Resveratrol, Pharmacokinetics, CYP3A1/2, CYP2C11

INTRODUCTION

Tofacitinib (Fig. 1A) is a Janus kinase (JAK) 1 and 3 inhibitor that blocks the JAK signal transducer and activator of the transcription (STAT) signaling pathway (Srivastava *et al*., 2018). It is used to treat rheumatoid arthritis (RA), particularly in cases where methotrexate is ineffective (Claxton *et al*., 2018; Fukuda *et al*., 2019). Approximately 70% of the oral dose of tofacitinib is metabolized by the hepatic microsomal cytochromes P450 (CYP) 3A4 and CYP2C19, with the remaining tofacitinib excreted unchanged by the kidneys. The terminal half-life of the drug is 3.2 h (Bannwarth *et al*., 2013; Dowty *et al*., 2014).

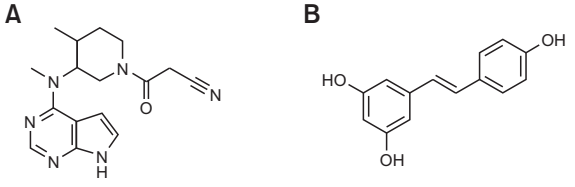

Fig. 1. Chemical structure of tofacitinib (A) and resveratrol (B).

Acetaminophen (APAP) is one of the most commonly used over-the-counter analgesic and antipyretic drugs (Yan *et al*., 2018). However, APAP overdose is also the leading cause of acute liver injury (ALI) (Budnitz *et al*., 2011). Excessive APAP administration saturates its normal metabolic pathways, leading to the accumulation of the hepatotoxic metabolite, N-acetyl-p-benzoquinone-imine (NAPQI) (Qian *et al*., 2021). NAPQI depletes glutathione (GSH) in hepatocytes and forms toxic adducts with cellular proteins, causing oxidative stress and cell death (Bunchorntavakul and Reddy, 2013). APAP is still widely used to relieve inflammatory pain in patients with RA, particularly in those who experience side effects from nonsteroidal anti-inflammatory drugs (Fitzcharles and Shir, 2011). Although the drug is safe in doses up to 2,000 mg per day, doses ex-

Open Access **https://doi.org/10.4062/biomolther.2024.184**

Received Oct 10, 2024 **Revised** Nov 13, 2024 **Accepted** Nov 18, 2024
Published Online Dec 13, 2024

***Corresponding Author**
E-mail: shkim67@ajou.ac.kr
Tel: +82-31-219-3451, Fax: +82-31-219-3435

ceeding this can often lead to liver damage (Popiolek *et al*., 2021), which can then affect the metabolism of co-administered drugs (Bollinger, 2017). Given that tofacitinib is primarily metabolized by the liver, liver function is a crucial consideration in patients with RA, as severe inflammatory reactions in the liver can occur (Bae *et al*., 2022).

Resveratrol (RVT, Fig. 1B) is a polyphenolic compound abundant in grape skins, wine, and peanuts, and is known for its antioxidant, anticancer, and anti-inflammatory effects (Mbimba *et al*., 2012). Additionally, the hepatoprotective effects of RVT are mediated through antioxidant (Zhang *et al*., 2015), anti-inflammatory (Jiang *et al*., 2016), anti-apoptotic (Shen *et al*., 2016), cell survival pathway activating (Baur and Sinclair, 2006), and antifibrotic effects (Gomez-Zorita *et al*., 2012). Recent studies have reported the hepatoprotective effects of RVT in APAP-induced ALI (Gokkaya *et al*., 2022). However, studies on the pharmacokinetic changes of drugs influenced by the hepatoprotective effects of RVT remain limited.

This study aims to demonstrate the hepatoprotective effect of RVT in an APAP-induced ALI rats through the pharmacokinetic changes of tofacitinib following intravenous and oral administration in ALI rats with or without RVT. In addition, this effect of RVT was also verified through the *in vitro* metabolic activity of tofacitinib and the protein expression changes of CYP isozymes involved in the metabolism of tofacitinib in the microsomes of the liver and intestine.

MATERIALS AND METHODS

Chemicals

Tofacitinib citrate, hydrocortisone (used as the internal standard for high-performance liquid chromatography [HPLC] analysis), and APAP were sourced from Sigma-Aldrich (St. Louis, MO, USA). RVT was procured from the Tokyo Chemical Industry (Tokyo, Japan). Ethyl acetate and acetonitrile, required for HPLC-based tofacitinib analysis, were supplied by J.T. Baker (Phillipsburg, NJ, USA), and β-cyclodextrin was obtained from Wako (Osaka, Japan). Primary antibodies targeting CYP3A1/2, CYP2E1, CYP2C11, CYP2D1, and CYP2BA1/2 were kindly provided by Detroit R&D Inc. (Detroit, MI, USA), while β-actin (used as a loading control) was sourced from Cell Signaling Technology (Beverly, MA, USA). All other chemicals were of HPLC or analytical grade and were used as received without further purification.

Animals

Seven-week-old male Sprague-Dawley rats, weighing 200-230 g, were obtained from DBL (Incheon, Korea). Animals were housed individually under controlled conditions at the Laboratory Animal Research Center, Ajou University Medical Center (Suwon, Korea). Environmental conditions were regulated at 21-23°C with 45-55% relative humidity and a 12-h light/dark cycle (07:00-19:00/19:00-07:00). Rats had unrestricted access to food and water. All experimental procedures adhered to the approved protocols of the Institutional Animal Care and Use Committee (IACUC No. 2023-0082) at the Laboratory Animal Research Center, Ajou University Medical Center.

Induction of ALI

Rats were randomly assigned to four groups: control (CON), RVT, ALI, and ALI-RVT. ALI was induced by administering a single intraperitoneal injection of APAP (400 mg/kg) dissolved in phosphate-buffered saline (PBS) (Du *et al*., 2015). The RVT group received a single intraperitoneal injection of RVT (50 mg/kg) dissolved in 40% dimethyl sulfoxide (DMSO) in saline (Du *et al*., 2015). In the ALI-RVT group, 50 mg/kg RVT was injected intraperitoneally 1.5 h before APAP administration (Du *et al*., 2015; Wang *et al*., 2015). The control group was treated with PBS only. Rats were euthanized for tissue collection or surgery 24 h after APAP injection (Elbe *et al*., 2018).

Biochemical profile analysis and tissue microscopy

Plasma and 24-h urine samples were collected from the four groups of rats: CON, RVT, ALI, and ALI-RVT (n=3 per group). Plasma levels of albumin, blood urea nitrogen (BUN), glutamate pyruvate transaminase (GPT), glutamate oxaloacetate transaminase (GOT), serum creatinine (S_{CR}), and total protein were analyzed (Green Cross Reference Lab, Seoul, Korea). Urine volume and creatinine concentration were measured to calculate creatinine clearance (CL_{CR}), as previously outlined (Choi *et al*., 2024). Liver and kidney weights were also recorded. For histopathological analysis, liver and kidney tissue sections were fixed in 10% formalin for biopsy.

Rat plasma protein binding of tofacitinib

The plasma protein binding of tofacitinib was assessed using freshly isolated plasma from the CON, RVT, ALI, and ALI-RVT groups (n=3 per group). Ultrafiltration was performed following a method similar to that previously described (Barre *et al*., 1985). Briefly, rat plasma spiked with 5 μg/mL of tofacitinib was added to a Nanosep 10 K centrifugal filter unit (Pall Co., Ann Arbor, MI, USA) and centrifuged at 1,500 × g for 30 min. A 100-μL sample of the ultrafiltrate, containing the unbound fraction of tofacitinib, was then frozen at –80°C until HPLC analysis was performed (Kim *et al*., 2020). To account for non-specific binding to the filtration device, PBS (pH 7.4) containing an equivalent concentration of tofacitinib was subjected to the same conditions (n=3). The percentage of tofacitinib bound to plasma proteins was determined using the following formula:

$$\text{Binding } \% = \frac{C_T - C_F}{C_T} \times 100 \quad (1)$$

where C_F represents the concentration of the unbound drug in the ultrafiltrate and C_T is the total drug concentration initially added to the ultrafiltration unit (Barre *et al*., 1985).

Intravenous and oral administration of tofacitinib in rats

The procedures for intravenous and oral administration, as well as rat pretreatment, were performed following previously established methods (Bae *et al*., 2020; Kim *et al*., 2020; Choi *et al*., 2024). The cannulae were inserted into the carotid artery for blood collection and into the jugular vein for drug administration. After cannulation, the rats were allowed a recovery period of 3-4 h before starting the experiments. The rats were allowed to move freely throughout the experiment.

For intravenous administration, tofacitinib (10 mg/kg), dissolved in saline containing 0.5% β-cyclodextrin, was injected into the jugular vein over 1 min in the CON (n=6), RVT (n=6), ALI (n=7), and ALI-RVT (n=7) groups. Blood samples were

collected from the carotid artery at 0 (pre-dose), 1, 5, 15, 30, 45, 60, 90, 120, 180, 240, and 360 min. Tofacitinib (20 mg/kg) was orally administered to CON (n=6), RVT (n=6), ALI (n=6), and ALI-RVT (n=7) rats, and blood was collected at 0 (pre-dose), 5, 15, 30, 45, 60, 90, 120, 180, 240, 360, 480, 600, and 720 min. Blood samples were centrifuged, and 50 μL of plasma was stored at –80°C until HPLC analysis of tofacitinib was performed (Kim *et al*., 2020). At 24-h, urine output over 24 h and the entire gastrointestinal tract were collected following the methods described in previous studies (Lee and Kim, 2019; Choi *et al*., 2024). After measuring the total volume of urine, a 100-μL aliquot of both urine and gastrointestinal samples was taken and stored at –80°C until HPLC analysis (Kim *et al*., 2020).

Determination of the V_{max}, K_m, and CL_{int}

Hepatic and intestinal microsomes were prepared according to previously established methods (Duggleby, 1995; Choi *et al*., 2024). The *in vitro* metabolic activity was evaluated using microsomes extracted from the liver and intestines of rats in the CON, RVT, ALI, and ALI-RVT groups (n=3 per group). Microsomal protein concentrations were quantified using bicinchoninic acid assay. The *in vitro* system consisted of 1 mg of microsomal protein, 1 μL of DMSO containing tofacitinib (5, 10, 20, 50, 100, 200, and 500 μM), and a nicotinamide adenine dinucleotide phosphate hydrogen (NADPH)-generating system (Corning Inc., Corning, NY, USA). To this, 0.1 M PBS (pH 7.4) was added for a final volume of 1 mL. The reaction mixture was incubated in a water bath shaker at 37°C with 50 oscillations per minute for 15 min. The reaction was stopped by adding methanol at a volume twice that of the reaction mixture. The kinetic parameters, including the maximum reaction velocity (V_{max}) and the apparent Michaelis-Menten constant (K_m, the substrate concentration at which the reaction rate is half of V_{max}), were determined using nonlinear regression analysis (Duggleby, 1995; Bae *et al*., 2022; Choi *et al*., 2024). The intrinsic clearance (CL_{int}) of tofacitinib was calculated by dividing V_{max} by K_m (Duggleby, 1995; Bae *et al*., 2022; Choi *et al*., 2024).

Immunoblot analysis

Microsomal proteins from liver and intestinal tissues (30-50 μg per lane) were separated using 10% sodium dodecyl sulfate-polyacrylamide gel electrophoresis (SDS-PAGE) and subsequently transferred onto membranes. The membranes were incubated at 4°C overnight with primary antibodies (diluted 1:2,000) targeting CYP2B1/2, CYP2C11, CYP2D1, CYP3A1/2, and β-actin. The membranes were then incubated with a secondary antibody (diluted 1:10,000) for 1 h at room temperature. Protein bands were visualized using enhanced chemiluminescence and their intensities were analyzed using ImageJ 1.45s software (NIH, Bethesda, MD, USA).

HPLC analysis

Biological samples for HPLC analysis of tofacitinib were prepared according to previously described methods (Kim *et al*., 2020). A 50 μL aliquot from each sample was mixed with 20% ammonia solution (20 μL) containing hydrocortisone (10 μg/mL) as the internal standard, followed by extraction with ethyl acetate (750 μL). The organic layer was then evaporated under a nitrogen stream. The residue was then re-dissolved, and 50 μL of the resulting supernatant was injected onto a C_{18} reversed-phase column (250×4.6 mm, 5 μm; Young Jin Biochrom, Seongnam, Korea) for analysis using a Prominence LC-20A HPLC system (Shimadzu, Kyoto, Japan) equipped with a UV detector set to 287 nm. The mobile phase consisted of 10 mM ammonium acetate buffer (pH 5.0) and acetonitrile at a ratio of 69.5:30.5 (v/v), at a flow rate of 1 mL/min. The retention times of tofacitinib and hydrocortisone were approximately 7.2 min and 11.3 min, respectively. The lower limits of quantification for tofacitinib in rat plasma and urine were determined to be 0.01 and 0.1 μg/mL, respectively. The intraday precision (coefficient of variation) for rat plasma and urine ranged from 3.69% to 5.88% and from 4.21% to 6.18%, respectively. The inter-day precision values were 5.06% for plasma and 5.46% for urine (Kim *et al*., 2020).

Pharmacokinetic analysis

Pharmacokinetic parameters were calculated using the standard approach outlined by Gibaldi and Perrier (1982) via non-compartmental analysis using WinNonlin software (Pharsight Co., Mountain View, CA, USA). The area under the plasma concentration-time curve (AUC) from time zero to infinity was estimated using the trapezoidal rule with extrapolation (Chiou, 1978). The peak plasma concentration (C_{max}) and time to reach C_{max} (T_{max}) were determined directly from the plasma concentration-time profiles. The absolute oral bioavailability (F) of tofacitinib was calculated by taking the ratio of the dose-normalized AUC_{oral} to the dose-normalized $AUC_{intravenous}$, where AUC_{oral} refers to the AUC following oral administration, and $AUC_{intravenous}$ denotes the AUC following intravenous administration.

Statistical analysis

The data are expressed as mean ± standard deviation (SD). Analysis of variance (ANOVA) was performed to compare the four groups, followed by Tukey's post-hoc test. A p-value of less than 0.05 was deemed statistically significant.

RESULTS

Preliminary data and tissue microscopy

Fig. 2A illustrates the body weight, biochemical markers, plasma protein binding of tofacitinib, CL_{CR}, and relative liver and kidney weights across the four rat groups. Liver dysfunction in ALI rats was evidenced by a 71.8% increase in GOT and a 4.01% reduction in total protein, compared to the CON group. RVT treatment in ALI-RVT rats substantially improved liver function compared to ALI rats, leading to a 35.1% decrease in GOT and a 4.50% increase in total protein (Fig. 2A). Other indicators of liver function in ALI rats showed no major damage; albumin, GPT levels, and relative liver weight remained within normal ranges (Mitruka and Rawnsley, 1981), and were comparable among all groups. Similarly, renal function indicators, such as urea nitrogen, relative kidney weight, and CL_{CR}, were not impaired in ALI rats (Fig. 2A). Liver histology showed widespread tissue damage and extensive cell death in the ALI rats (Fig. 2B). However, kidney histology revealed no notable tissue damage. In ALI-RVT rats, RVT administration alleviated tissue damage, as no significant disturbances were detected in liver or kidney histology (Fig. 2B).

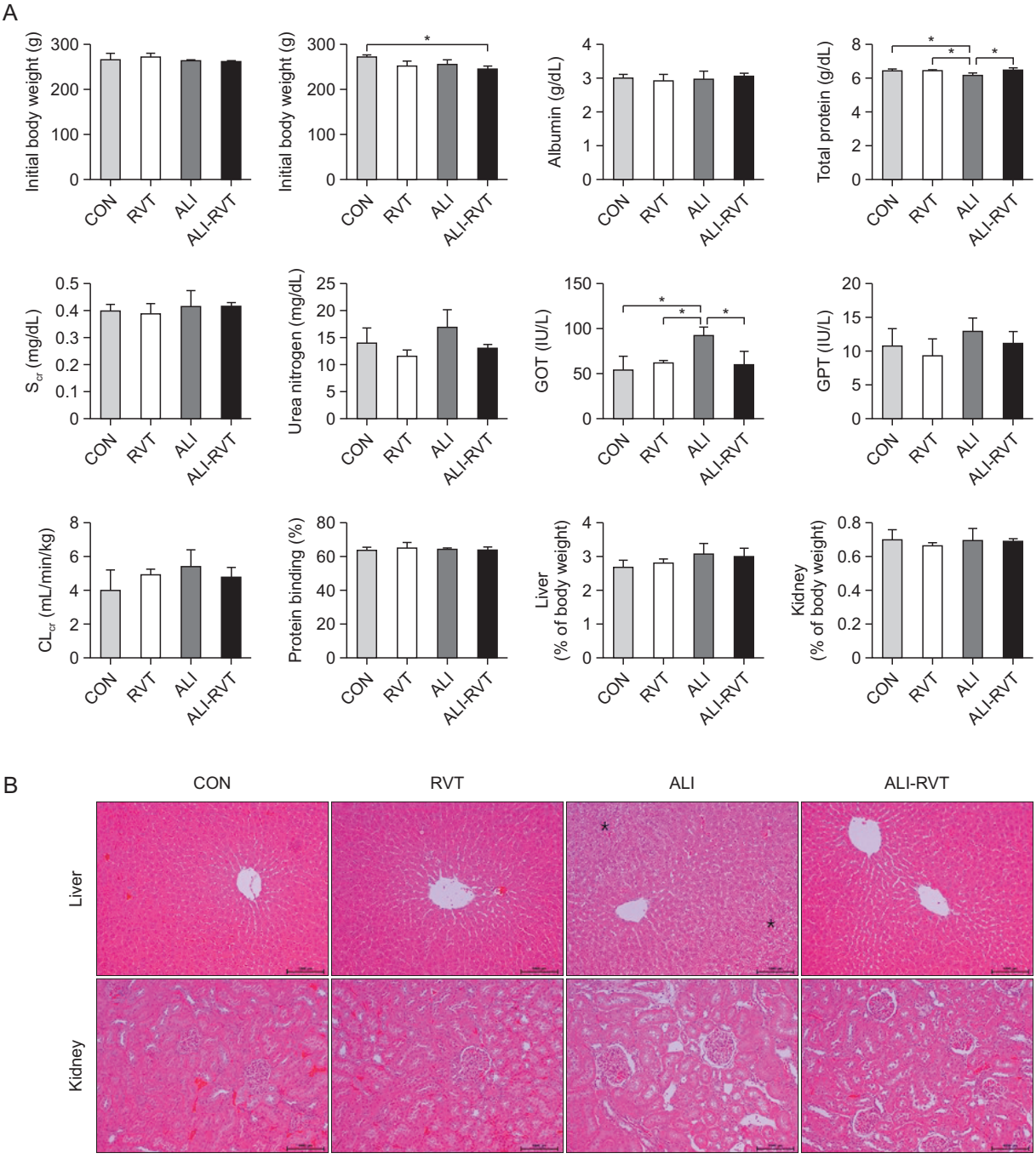

Fig. 2. (A) Body weight, plasma chemistry parameters, creatinine clearance (CLCR), plasma protein binding of tofacitinib, and relative liver and kidney weights in control (CON), resveratrol (RVT), acute liver injury (ALI), and acute liver injury-resveratrol (ALI-RVT) groups of rats. Data are presented as mean ± standard deviation (*n*=3 per group). (B) Liver and kidney histopathology in CON, RVT, ALI, and ALI-RVT groups. The asterisks mark areas of significant liver damage, characterized by extensive cell death. BUN, blood urea nitrogen; BW, body weight; GOT, glutamate oxaloacetate transaminase; GPT, glutamate pyruvate transaminase; SCR, serum creatinine concentration. *p<0.05. Scale bar=1,000 μm.

Plasma protein binding of tofacitinib

The plasma protein binding of tofacitinib was relatively stable across the CON, RVT, ALI, and ALI-RVT groups, with binding percentages of 63.7, 65.1, 64.2, and 63.6%, respectively (Fig. 2A). Additionally, the mean recovery rate of tofacitinib (5 μg/mL) in phosphate buffer following ultrafiltration was 99.7 ± 2.51% (*n*=3), suggesting minimal non-specific binding to the filtration apparatus.

Intravenous and oral administration of tofacitinib in rats

Fig. 3A shows the mean arterial plasma concentration–time profiles of tofacitinib after intravenous administration of 10 mg/kg in the CON, RVT, ALI, and ALI-RVT groups, along with the pharmacokinetic parameters listed in Table 1. Compared to the CON group, the ALI group showed significant alterations in tofacitinib pharmacokinetics, including a 207% increase in AUC, 113% increase in terminal half-life, and considerable reductions in CL, CL_{NR}, and CL_R (by 64.7%, 66.1%, and 70.8%, respectively). In the ALI-RVT rats, RVT administration notably improved all pharmacokinetic parameters, returning them to levels close to those in the CON group (Table 1). When comparing ALI and ALI-RVT rats, ALI-RVT rats exhibited a 62.0% reduction in AUC, 38.0% shorter terminal half-life, and significant increases in CL, CL_{NR}, and CL_R (by 142%, 141%, and 398%, respectively), along with an 117% increase in the percentage of drugs excreted in an unchanged form in the urine after 24 h ($Ae_{0\text{-}24}$ h). Pharmacokinetic comparisons between the CON and RVT rats showed no significant differences.

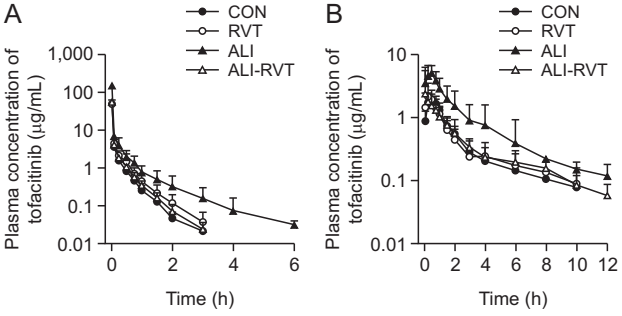

Fig. 3. Mean arterial plasma concentration-time profiles of tofacitinib after (A) 1-min intravenous infusion (10 mg/kg) in four groups of rats: control (CON, *n*=6), resveratrol (RVT, *n*=6), acute liver injury (ALI, *n*=7) and acute liver injury-resveratrol (ALI-RVT, *n*=7) rats. (B) After oral administration of tofacitinib (20 mg/kg) to CON (*n*=6), RVT (*n*=6), ALI (*n*=6) and ALI-RVT (*n*=7) rats. Data are displayed as mean ± standard deviation.

Fig. 3B illustrates the mean arterial plasma concentration–time curves for tofacitinib after oral administration of 20 mg/kg in the four groups. Pharmacokinetic parameters such as AUC, CL_R, and $Ae_{0\text{-}24}$ h for tofacitinib are summarized in Table 2. Compared to CON rats, ALI rats showed an 161% increase in AUC and a 76.4% decrease in CL_R. However, ALI-RVT rats demonstrated notable improvements in pharmacokinetics, with values closer to those observed in CON rats. Specifically, the AUC decreased by 41.4%, whereas the CL_R increased by 211%. The *F* values were similar across the four groups, and no significant differences in the pharmacokinetic parameters were observed between the CON and RVT rats (Table 2).

In vitro metabolism of tofacitinib

Fig. 4A illustrates the V_{max}, K_m, and CL_{int} values for the metabolism of tofacitinib in hepatic microsomes across the four experimental groups. The V_{max} in ALI rats showed a pronounced reduction of 58.9% compared to that in the CON group. In contrast, the administration of RVT to ALI-RVT rats partially restored V_{max} to 85.1% of the value observed in CON rats. K_m values remained consistent across all groups, indicating that the affinity of the enzyme for tofacitinib remained unchanged. As a result, CL_{int} in ALI rats was 69.6% lower than that in CON rats, but was restored to 93.1% of CON values following RVT administration in the ALI-RVT group. These observations suggest that the hepatic metabolism of tofacitinib was impaired in ALI rats and improved upon co-administration of RVT.

In Fig. 4B, the V_{max}, K_m, and CL_{int} values for tofacitinib metabolism in the intestinal microsomes are shown. Unlike hepatic microsomes, no significant differences in V_{max}, K_m, and CL_{int} were observed across the four groups. This indicated that neither APAP-induced ALI nor RVT treatment affected the metabolism of tofacitinib in intestinal microsomes.

Expression of CYP isozymes

The hepatic and intestinal CYP isozyme expression levels

Table 1. Mean pharmacokinetic parameters (± standard deviation) of tofacitinib after its intravenous administration at a dose of 10 mg/kg to CON, RVT, ALI, and ALI-RVT rats

Parameters	Intravenous			
	CON (*n*=6)	RVT (*n*=6)	ALI (*n*=7)	ALI-RVT (*n*=7)
Body weight (g)	279 ± 5.71	259 ± 4.62	256 ± 4.22	245 ± 5.15
Terminal half-life (min)	22.7 ± 7.92	28.4 ± 11.8	48.4 ± 15.6*	30.0 ± 6.44
AUC (μg · min/mL)	244 ± 26.8	278 ± 12.4	749 ± 182*	285 ± 23.9
CL (mL/min/kg)	41.3 ± 4.92	36.0 ± 1.64	14.6 ± 8.18*	35.3 ± 2.74
CL_R (mL/min/kg)	2.19 ± 0.756	2.63 ± 1.11	0.653 ± 0.510*	3.25 ± 1.17
CL_{NR} (mL/min/kg)	39.2 ± 4.76	33.4 ± 2.00	13.3 ± 2.68*	32.1 ± 2.96
V_{ss} (mL/kg)	393 ± 171	604 ± 311	187 ± 65.5	387 ± 107
$Ae_{0\text{-}24\ h}$ (% of dose)	5.30 ± 1.91	7.31 ± 3.12	4.26 ± 2.87	9.25 ± 3.62
$GI_{24\ h}$ (% of dose)	0.108 ± 0.0444	0.147 ± 0.00805	0.134 ± 0.0339	0.115 ± 0.0493

$Ae_{0\text{-}24\ h}$, the percentage of drug excreted as an unchanged form in the urine for 24 h; ALI, acute liver injury; ALI-RVT, acute liver injury-resveratrol; AUC, area under plasma concentration-time curves from time zero to time infinity; CL, time-averaged total body clearance; CL_{NR}, time-averaged non-renal clearance; CL_R, time-averaged renal clearance; CON, control; $GI_{24\ h}$, the percentage of drug remaining in the gastrointestinal tract at 24 h; RVT, resveratrol; V_{ss}, the apparent volume of distribution at steady state.

*ALI is significantly different from CON, RVT and ALI-RVT (p<0.05).

Statistical results was obtained from analysis of variance (ANOVA) followed by Tukey's post-hoc test. A detailed statistical result is found in Supplimentary Table 1.

Table 2. Mean pharmacokinetic parameters (± standard deviation) of tofacitinib after its oral administration at a dose of 20 mg/kg to CON, RVT, ALI, and ALI-RVT rats

Parameters	Oral			
	CON (*n*=6)	RVT (*n*=6)	ALI (*n*=6)	ALI-RVT (*n*=7)
Body weight (g)	231 ± 4.02	231 ± 4.72	231 ± 6.38	236 ± 5.99
AUC (μg · min/mL)	214 ± 26.0	241 ± 51.4	602 ± 200*	353 ± 111
C_{max} (μg/mL)	2.18 ± 0.545	2.49 ± 0.921	5.44 ± 1.81	2.78 ± 3.69
T_{max} (min)	27.5 ± 11.3	27.5 ± 17.5	25.0 ± 6.38	20.7 ± 12.1
CL_R (mL/min/kg)	5.29 ± 1.24	4.13 ± 2.69	1.25 ± 0.875*	3.89 ± 0.598
$Ae_{0\text{-}24\ h}$ (% of dose)	4.72 ± 2.03	3.96 ± 2.11	3.04 ± 1.74	6.41 ± 1.86
$GI_{24\ h}$ (% of dose)	0.791 ± 1.06	0.295 ± 0.0618	0.743 ± 0.917	0.467 ± 0.243
F (%)	43.9	43.3	40.2	61.9

$Ae_{0\text{-}24\ h}$, the percentage of drug excreted as an unchanged form in the urine for 24 h; ALI, acute liver injury; ALI-RVT, acute liver injury-resveratrol; AUC, area under plasma concentration-time curves from time zero to time infinity; C_{max}, maximum plasma concentration; CL_R, time-averaged renal clearance; CON, control; *F*, absolute oral bioavailability; $GI_{24\ h}$, the percentage of drug remaining in the gastrointestinal tract at 24 h; RVT, resveratrol; T_{max}, time to reach C_{max}.

*ALI is significantly different from CON, RVT and ALI-RVT (p<0.05).

Statistical results was obtained from analysis of variance (ANOVA) followed by Tukey's post-hoc test. A detailed statistical result is found in Supplimentary Table 2.

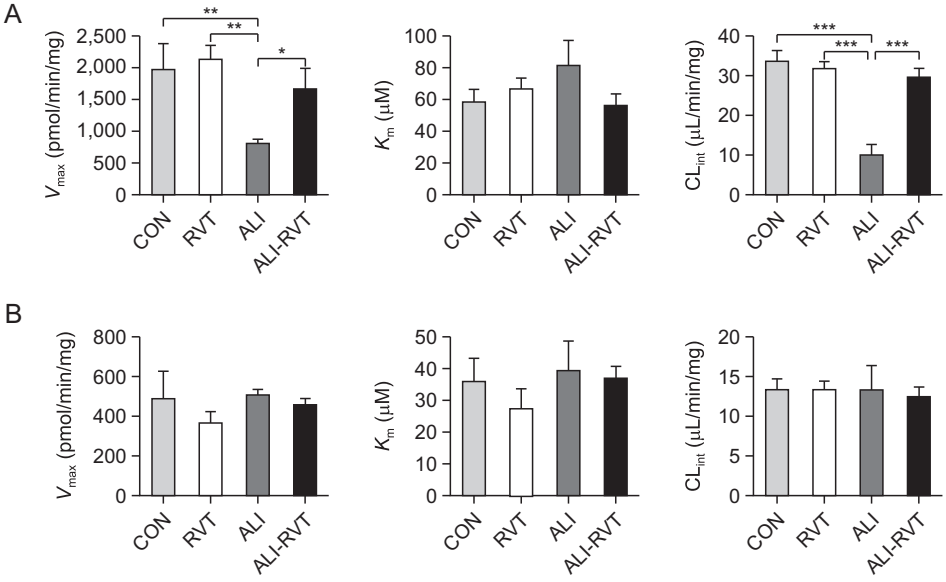

Fig. 4. Mean values of Vmax, Km and CL_{int} for tofacitinib metabolism in microsomes isolated from (A) liver and (B) intestines of rats from the following groups; control (CON, white), resveratrol (RVT), acute liver injury (ALI) and acute liver injury-resveratrol (ALI-RVT) rats (n=3 per group). This experiment was completed three times. Data are shown as mean ± standard deviation. Vmax, maximum velocity; Km, apparent Michaelis–Menten constant; CL_{int}, intrinsic clearance. *p<0.05; **p<0.01; ***p<0.001

in microsomes from CON, RVT, ALI, and ALI-RVT rats are shown in Fig. 5. In the hepatic microsomes of ALI rats, the expression levels of CYP2B1/2, CYP2C11, and CYP3A1/2 decreased by 24.3%, 58.3%, and 39.2%, respectively, compared to those in CON rats. However, in ALI-RVT rats, CYP2C11 expression increased by 41.5%, whereas CYP3A1/2 levels decreased by 35.9% compared with those in ALI rats. Unlike the liver findings, the intestinal microsomes of ALI rats showed elevated CYP2C11 and CYP3A1/2 levels, which were increased by 16.0% and 120%, respectively, compared to those in CON rats. Additionally, the expression of all CYP isozymes in intestinal microsomes was higher in ALI-RVT rats than in ALI rats. These findings suggest that ALI significantly affects CYP isozyme levels in both the hepatic and intestinal tissues, potentially leading to reduced hepatic metabolism of tofacitinib. RVT treatment appeared to counteract these alterations, bringing CYP isozyme expression in both the liver and intestines closer to the levels observed under non-ALI conditions.

DISCUSSION

An APAP overdose is a common cause of ALI, accounting for 10-30% of ALI cases, making it a significant contributor to

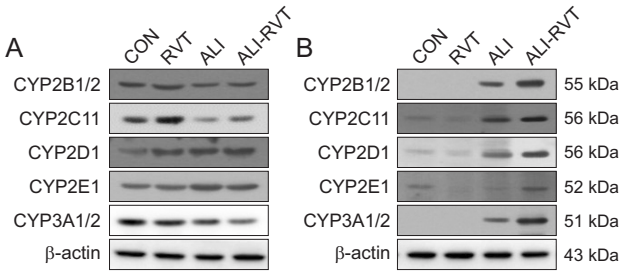

Fig. 5. Immunoblot analyses was conducted to evaluate cytochrome P450 (CYP) 2B1/2, CYP2C11, CYP2D1, CYP2E1, and CYP3A1/2 isozymes of hepatic (A) and intestinal (B) microsomes from control (CON), resveratrol (RVT), acute liver injury (ALI) and acute liver injury-resveratrol (ALI-RVT) rats. β-actin served as a loading control for normalization. This experiment was repeated three times, and band density was quantified using ImageJ 1.45s software (NIH).

drug-induced liver damage (Ahn, 2006). High doses of APAP result in increased production of its toxic intermediate metabolite, NAPQI, which is usually neutralized by GSH and excreted through urine (Mossanen and Tacke, 2015). However, once GSH stores are depleted, excess NAPQI binds to mitochondrial proteins within the hepatocytes, leading to cellular damage and hepatocellular necrosis (Jaeschke *et al*., 2020). Natural products offer potential protection against drug-induced liver damage, including that resulting from APAP overdose. RVT, a polyphenolic compound, has been shown to mitigate ALI (Sener *et al*., 2006), and pterostilbene, a compound in the same family, has demonstrated protective effects against APAP-induced liver injury (Fan *et al*., 2018).

In preliminary studies, the administration of RVT in ALI-RVT rats led to significant improvements in liver function compared to that in ALI rats, with key liver function markers, such as GOT and total protein levels and liver histology, trending towards baseline levels in the CON group (Fig. 2). This suggests that RVT may mitigate APAP-induced liver damage and exert hepatoprotective effects. APAP overdose is known to induce severe oxidative stress in liver tissues, causing GSH depletion and triggering oxidative injury, which is often associated with neutrophil infiltration (Guo *et al*., 2021). RVT counteracts oxidative stress, reduces neutrophil infiltration in tissues, inhibits hepatocellular death, and promotes liver regeneration by modulating the SIRT1/p53 signaling pathway (Sener *et al*., 2006; Wang *et al*., 2015). The reduction in final body weight in RVT rats is due to the conversion of white adipocytes into brown fat, which promotes liver fat reduction and weight loss (Zhou *et al*., 2019). For this reason, despite the improvement in liver function in ALI-RVT rats, their weight appears to have decreased even more than that of ALI rats. Consequently, our findings suggest that RVT protects against oxidative injury in liver tissues and limits neutrophil accumulation, thereby contributing to the protective effects observed in ALI-RVT rats.

Tofacitinib exhibits dose-independent linear pharmacokinetics when administered intravenously or orally in the dose range of 10-50 mg/kg (Lee and Kim, 2019). Accordingly, the intravenous and oral doses were set at 10 and 20 mg/kg, respectively. The substantial increase in AUC after intravenous tofacitinib administration in ALI rats was likely due to a significant reduction in CL compared to that in the CON group (Table 1). As the liver plays a central role in tofacitinib metabolism, the decrease in CL can be attributed to a reduction in CL_{NR}, which reflects metabolic clearance (Dowty *et al*., 2014; Lee and Kim, 2019). Considering that gastrointestinal and biliary excretion contribute minimally to tofacitinib clearance and that the drug remains chemically stable in gastric juice with limited enzymatic degradation (Kim *et al*., 2020), the observed reduction in CL_{NR} likely represents impaired hepatic metabolism of tofacitinib (Table 1).

Overdose with APAP depletes GSH and elevates reactive oxygen species (ROS) production owing to the accumulation of the toxic metabolite NAPQI, which leads to inflammation and liver damage (Al Humayed *et al*., 2020; Xu and Wang, 2023). This damage significantly impairs tofacitinib metabolism, which is primarily mediated by hepatic CYP3A1/2 and CYP2C11 in rats (Lee and Kim, 2019). In the ALI rats, this resulted in a marked reduction in CL_{NR}, which was considerably slower than that in the CON rats (Table 1). Tofacitinib has an intermediate hepatic extraction ratio of approximately 42.0% in rats (Lee and Kim, 2019), indicating that its hepatic clearance is primarily influenced by CL_{int} and the fraction of unbound drug in the plasma, rather than by hepatic blood flow (Wilkinson and Shand, 1975). As the plasma protein binding of tofacitinib remained unchanged between ALI and CON rats, the reduced CL_{NR} in ALI rats was likely attributable to a significant decrease in CL_{int} rather than to alterations in the unbound fraction of the drug. Supporting this hypothesis, the protein expression of hepatic CYP3A1/2 and CYP2C11 in ALI rats was diminished, and hepatic CL_{int} was significantly reduced. However, following RVT treatment in ALI-RVT rats, pharmacokinetic parameters such as AUC, CL, and CL_{NR} recovered to levels similar to those observed in CON rats. Interestingly, while RVT treatment restored overall drug metabolism, it selectively influenced different CYP isozymes; CYP2C11 expression increased, while CYP3A1/2 expression decreased, compared to those in ALI rats. This selective modulation may indicate that RVT exerts an inhibitory effect on CYP3A1/2 expression, which was observed not only in ALI-RVT rats but also in RVT rats, where CYP3A expression slightly decreased following RVT administration. The inhibition of CYP3A1/2 could have implications for drug interactions and the metabolic processing of compounds when co-administered with APAP (Hyrsova *et al*., 2019). In contrast, RVT administration upregulated CYP2C11 expression in ALI-RVT rats, which contributed to the recovery of hepatic enzyme activity to levels comparable to those in CON rats. This restoration of CYP2C11 expression likely enhances the key metabolic pathways for tofacitinib, resulting in the normalization of its pharmacokinetic parameters. In conclusion, RVT appears to offer significant hepatoprotective effects against APAP-induced liver damage, which, in turn, positively affects the pharmacokinetics of tofacitinib. By mitigating the adverse effects of liver injury, RVT treatment in ALI-RVT rats led to pharmacokinetic parameters, such as AUC, CL, and CL_{NR}, that closely resembled those of CON rats, underscoring the therapeutic potential of RVT in liver protection and its role in modulating drug metabolism.

After the oral administration of tofacitinib to ALI rats, the significantly greater AUC compared to that in CON rats suggests that reduced clearance, particularly CL_R, plays a critical role in this increase. Gastrointestinal absorption of tofacitinib was nearly complete in both CON and ALI rats, as evidenced by $GI_{24\ h}$ values representing less than 0.791% that of the oral dose; however, the increased AUC in ALI rats cannot be explained

solely by changes in absorption. Instead, the marked reduction in CL_R in ALI rats likely led to a decreased elimination rate, thereby contributing to the observed increase in AUC. However, the expression of intestinal CYP3A1/2 and CYP2C11 was higher in ALI rats than in CON rats. This pattern aligns with the findings in other models, such as cisplatin-induced renal failure, in which intestinal CYP isozyme expression increases (Bae *et al*., 2020; Choi *et al*., 2024). This phenomenon may be attributed to the higher sensitivity and instability of intestinal microsomes, as previously reported (Bruyère *et al*., 2009). Furthermore, there were no significant differences in CL_{int} among the four groups in the intestinal microsomes, suggesting that APAP-induced hepatotoxicity did not affect the intestinal metabolism of tofacitinib. This lack of intestinal involvement in tofacitinib metabolism aligns with the understanding that the toxic effects of APAP primarily target the liver rather than the gastrointestinal system. Hence, changes in tofacitinib pharmacokinetics in ALI rats are more closely associated with hepatotoxicity than with gastrointestinal factors. The increased expression of CYP3A1/2 and CYP2C11 in intestinal microsomes is not exactly known, however, these changes do not appear to significantly affect the overall tofacitinib metabolism in the gastrointestinal tract.

In a rat model of CCl_4-induced ALI, the metabolic activities of hepatic CYP3A1/2 and CYP2C11 were significantly reduced by 25% and 76%, respectively, indicating that liver injury substantially impairs the function of these CYP isozymes (Tan *et al*., 2008). This finding is consistent with the results observed in the APAP-induced ALI rat model, in which diminished CYP isozyme activity was also observed. Such reductions in the levels of liver CYP enzymes are common across different liver injury models. In clinical settings, a study demonstrated that the AUC of tofacitinib increased by 72.6% in patients with hepatic impairment compared to that in healthy individuals after oral administration (10 mg) (Lawendy *et al*., 2014). This parallels preclinical findings, suggesting that impaired hepatic metabolism leads to slower elimination and higher systemic exposure to tofacitinib. These results emphasize the importance of considering dosage adjustments for tofacitinib in patients with liver injury to avoid potential toxicity and maintain therapeutic efficacy.

In summary, administration of RVT successfully restored hepatic CYP2C11 expression and enhanced CL_{int} in ALI-RVT rats, normalizing tofacitinib metabolism to levels comparable to those in CON rats. These findings underscore the need to consider drug interactions involving natural compounds in clinical settings, especially in patients with liver disease. Natural extracts containing RVT or other polyphenols may influence the plasma concentrations of concurrently administered drugs. Thus, incorporating RVT could not only provide liver protective effects but also help mitigate increases in plasma levels of co-administered medications resulting from liver damage, ultimately preventing adverse effects linked to elevated drug concentrations.

CONFLICT OF INTEREST

The authors declare no conflicts of interest.

ACKNOWLEDGMENTS

This work was partly supported by the Basic Science Research Program through a grant from the National Research Foundation of Korea (NRF) funded by the Ministry of Science and ICT (MSIT) (NRF-2021R1A2C1011142) and by the GRRC program of Gyeonggi province (GRRCAjou2023-B04), Korea.

REFERENCES

Ahn, B. M. (2006) Acetaminophen-induced acute liver failure. *J. Korean Med. Assoc.* **49**, 846-853.

Al Humayed, S., Al-Hashem, F., Haidara, M. A., El Karib, A. O., Kamar, S. S., Amin, S. N. and Al-Ani, B. (2020) Resveratrol pretreatment ameliorates p53-Bax axis and augments the survival biomarker B-cell lymphoma 2 modulated by paracetamol overdose in a rat model of acute liver injury. *Pharmacology* **105**, 39-46.

Bae, S. H., Chang, S. Y. and Kim, S. H. (2020) Slower elimination of tofacitinib in acute renal failure rat models: contribution of hepatic metabolism and renal excretion. *Pharmaceutics* **12**, 714.

Bae, S. H., Choi, H. G., Park, S. Y., Chang, S. Y., Kim, H. and Kim, S. H. (2022) Effects of isosakuranetin on pharmacokinetic changes of tofacitinib in rats with N-dimethylnitrosamine-induced liver cirrhosis. *Pharmaceutics* **14**, 2684.

Bannwarth, B., Kostine, M. and Poursac, N. (2013) A pharmacokinetic and clinical assessment of tofacitinib for the treatment of rheumatoid arthritis. *Expert Opin. Drug Metab. Toxicol.* **9**, 753-761.

Barré, J., Chamouard, J. M., Houin, G. and Tillement, J. P. (1985) Equilibrium dialysis, ultrafiltration, and ultracentrifugation compared for determining the plasma-protein-binding characteristics of valproic acid. *Clin. Chem.* **31**, 60-64.

Baur, J. A. and Sinclair, D. A. (2006) Therapeutic potential of resveratrol: the *in vivo* evidence. *Nat. Rev. Drug Discov.* **5**, 493-506.

Bollinger, E. (2017) The impact of liver disease on drug metabolism. In Surgical Procedures on the Cirrhotic Patient (B. Eghtesad and J. Fung, Eds.). Springer, Cham.

Bruyère, A., Declevès, X., Bouzom, F., Proust, L., Martinet, M., Walther, B. and Parmentier, Y. (2009) Development of an optimized procedure for the preparation of rat intestinal microsomes: comparison of hepatic and intestinal microsomal cytochrome P450 enzyme activities in two rat strains. *Xenobiotica* **39**, 22-32.

Budnitz, D. S., Lovegrove, M. C. and Crosby, A. E. (2011) Emergency department visits for overdoses of acetaminophen-containing products. *Am. J. Prev. Med.* **40**, 585-592.

Bunchorntavakul, C. and Reddy, K. R. (2013) Acetaminophen-related hepatotoxicity. *Clin. Liver Dis.* **17**, 587-607.

Chiou, W. L. (1978) Critical evaluation of the potential error in pharmacokinetic studies of using the linear trapezoidal rule method for the calculation of the area under the plasma level--time curve. *J. Pharmacokinet. Biopharm.* **6**, 539-546.

Choi, H. G., Park, S. Y., Bae, S. H., Chang, S. Y. and Kim, S. H. (2024) Loganinameliorates acute kidney injury and restores tofacitinib metabolism in rats: implications for renal protection and drug interaction. *Biomol. Ther. (Seoul)* **32**, 601-610.

Claxton, L., Taylor, M., Soonasra, A., Bourret, J. A. and Gerber, R. A. (2018) An economic evaluation of tofacitinib treatment in rheumatoid arthritis after methotrexate or after 1 or 2 TNF inhibitors from a U.S. payer perspective. *J. Manag. Care Spec. Pharm.* **24**, 1010-1017.

Dowty, M. E., Lin, J., Ryder, T. F., Wang, W., Walker, G. S., Vaz, A., Chan, G. L., Krishnaswami, S. and Prakash, C. (2014) The pharmacokinetics, metabolism, and clearance mechanisms of tofacitinib, a janus kinase inhibitor, in humans. *Drug Metab. Dispos.* **42**, 759-773.

Du, K., McGill, M, R., Xie, Y., Bajt, M, L. and Jaeschke, H. (2015) Resveratrol prevents protein nitration and release of endonucleases from mitochondria during acetaminophen hepatotoxicity. *Food Chem.Toxicol.* **81**, 62-70.

Duggleby, R. G. (1995) Analysis of enzyme progress curves by nonlin-

ear regression. *Methods Enzymol.* **249**, 61-90.
Elbe, H., Gul, M., Cetin, A., Taslidere, E., Ozyalin, F., Turkoz, Y. and Otlu, A. (2018) Resveratrol reduces light and electron microscopic changes in acetaminophen-induced hepatotoxicity in rats: role of iNOS expression. *Ultrastruct. Pathol.* **42**, 39-48.
Fan, X., Wang, L., Huang, J., Lv, H., Deng, X. and Ci, X. (2018) Pterostilbene reduces acetaminophen-induced liver injury by activating the Nrf2 antioxidative defense system via the AMPK/Akt/GSK3β pathway. *Cell. Physiol. Biochem.* **49**, 1943-1958.
Fitzcharles, M. A. and Shir, Y. (2011) Management of chronic pain in the rheumatic diseases with insights for the clinician. *Ther. Adv. Musculoskelet. Dis.* **3**, 179-190.
Fukuda, T., Naganuma, M. and Kanai, T. (2019) Current new challenges in the management of ulcerative colitis. *Intest. Res.* **17**, 36-44.
Gibaldi, M. and Perrier, D. (1982) Pharmacokinetics, 2nd ed. Marcel-Dekker, New York.
Gokkaya, E. O., Yesilot, S., Ozgocmen, M., Aslankoc, R. and Aydin Acar, C. (2022) Protective effects of resveratrol and avocado oil against paracetamol-induced hepatotoxicity in rats. *Drug Chem. Toxicol.* **45**, 2131-2139.
Gómez-Zorita, S., Fernández-Quintela, A., Macarulla, M. T., Aguirre, L., Hijona, E., Bujanda, L., Milagro, F., Martínez, J. A. and Portillo, M. P. (2012) Resveratrol attenuates steatosis in obese Zucker rats by decreasing fatty acid availability and reducing oxidative stress. *Br. J. Nutr.* **107**, 202-210.
Guo, H., Chen, S., Xie, M., Zhou, C. and Zheng, M. (2021) The complex roles of neutrophils in APAP-induced liver injury. *Cell Prolif.* **54**, e13040.
Hyrsova, L., Vanduchova, A., Dusek, J., Smutny, T., Carazo, A., Maresova, V., Trejtnar, F., Barta, P., Anzenbacher, P., Dvorak, Z. and Pavek, P. (2019) Trans-resveratrol, but not other natural stilbenes occurring in food, carries the risk of drug-food interaction via inhibition of cytochrome P450 enzymes or interaction with xenosensor receptors. *Toxicol. Lett.* **300**, 81-91.
Jaeschke, H., Akakpo, J. Y., Umbaugh, D. S. and Ramachandran, A. (2020) Novel therapeutic approaches against acetaminophen-induced liver injury and acute liver failure. *Toxicol. Sci.* **174**, 159-167.
Jiang, L., Zhang, L., Kang, K., Fei, D., Gong, R., Cao, Y., Pan, S., Zhao, M. and Zhao, M. (2016) Resveratrol ameliorates LPS-induced acute lung injury via NLRP3 inflammasome modulation. *Biomed. Pharmacother.* **84**, 130-138.
Kim, J. E., Park, M. Y. and Kim, S. H. (2020) Simple determination and quantification of tofacitinib, a JAK inhibitor, in rat plasma, urine and tissue homogenates by HPLC and its application to a pharmacokinetic study. *J. Pharm. Investig.* **50**, 603-612.
Lawendy, N., Lamba, M., Chan, G., Wang, R., Alvey, C, W. and Krishnaswami, S. (2014) The effect of mild and moderate hepatic impairment on the pharmacokinetics of tofacitinib, an orally active Janus kinase inhibitor. *Clin. Pharmacol. Drug Dev.* **3**, 421-427.
Lee, J. S. and Kim, S. H. (2019) Dose-dependent pharmacokinetics of tofacitinib in rats: influence of hepatic and intestinal first-pass metabolism. *Pharmaceutics* **11**, 318.
Mbimba, T., Awale, P., Bhatia, D., Geldenhuys, W, J., Darvesh, A, S., Carroll, R, T. and Bishayee, A. (2012) Alteration of hepatic proinflammatory cytokines is involved in the resveratrol-mediated chemoprevention of chemically-induced hepatocarcinogenesis. *Curr. Pharm. Biotechnol.* **13**, 229-234.
Mitruka, B. M. and Rawnsley, H. M. (1981) Clinical Biochemical and Hematological Reference Values in Normal Experimental Animals and Normal Humans, 2nd ed. Masson Publishing USA Inc., New York.
Mossanen, J. C. and Tacke, F. (2015) Acetaminophen-induced acute liver injury in mice. *Lab. Anim.* **49**, 30-36.
Popiolek, I., Hydzik, P., Jagielski, P., Zrodlowska, M., Mystek, K. and Porebski, G. (2021) Risk factors for hepatotoxicity due to paracetamol overdose in adults. *Medicina (Kaunas)* **57**, 752.
Qian, H., Bai, Q., Yang, X., Akakpo, J. Y., Ji, L., Yang, L., Rülicke, T., Zatloukal, K., Jaeschke, H., Ni, H. M. and Ding, W. X. (2021) Dual roles of p62/SQSTM1 in the injury and recovery phases of acetaminophen-induced liver injury in mice. *Acta Pharm. Sin. B* **11**, 3791-3805.
Sener, G., Toklu, H. Z., Sehirli, A. O., Velioğlu-Oğünç, A., Cetinel, S. and Gedik, N. (2006) Protective effects of resveratrol against acetaminophen-induced toxicity in mice. *Hepatol. Res.* **35**, 62-68.
Shen, C., Cheng, W., Yu, P., Wang, L., Zhou, L., Zeng, L. and Yang, Q. (2016) Resveratrol pretreatment attenuates injury and promotes proliferation of neural stem cells following oxygen-glucose deprivation/reoxygenation by upregulating the expression of Nrf2, HO-1 and NQO1 *in vitro*. *Mol. Med. Rep.* **14**, 3646-3654.
Srivastava, A., Ståhle, M., Pivarcsi, A., and Sonkoly, E. (2018) Tofacitinib represses the januskinase-signal transducer and activators of transcription signallingpathway in keratinocytes. *Acta Derm. Venereol.* **98**, 772-775.
Tan, W., Wang, B., Zhao, J., Sheng, L., Hu, J. and Li, Y. (2008) Pharmacokinetics of bicyclol in rats with acute hepatic failure. *Xenobiotica* **38**, 1399-409.
Wang, Y., Jiang, Y., Fan, X., Tan, H., Zeng, H., Wang, Y., Chen, P., Huang, M. and Bi, H. (2015) Hepato-protective effect of resveratrol against acetaminophen-induced liver injury is associated with inhibition of CYP-mediated bioactivation and regulation of SIRT1-p53 signaling pathways. *Toxicol. Lett.* **236**, 82-89.
Wilkinson, G. R. and Shand, D. G. (1975) A physiological approach to hepatic drug clearance. *Clin. Pharmacol. Ther.* **18**, 377-390.
Xu, L. and Wang, H. (2023) A dual role of inflammation in acetaminophen-induced liver injury. *Liver Res.* **7**, 9-15
Yan, M., Huo, Y., Yin, S. and Hu, H. (2018) Mechanisms of acetaminophen-induced liver injury and its implications for therapeutic interventions. *Redox Biol.* **17**, 274-283.
Zhang, Y., Chen, M. L., Zhou, Y., Yi, L., Gao, Y. X., Ran, L., Chen, S. H., Zhang, T., Zhou, X., Zou, D., Wu, B., Wu, Y., Chang, H., Zhu, J. D., Zhang, Q. Y. and Mi, M. T. (2015) Resveratrol improves hepatic steatosis by inducing autophagy through the cAMP signaling pathway. *Mol. Nutr. Food Res.* **59**, 1443-1457.
Zhou, L., Xiao, X., Zhang, Q., Zheng, J. and Deng, M. (2019) Deciphering the anti-obesity benefits of resveratrol: the "gut microbiota-adipose tissue" axis. *Front. Endocrinol. (Lausanne)* **10**, 413.